ARTICLE
Journal of Cellular Biochemistry 111:391–401 (2010)

Journal of Cellular Biochemistry

OCT3/4 Regulates Transcription of Histone Deacetylase 4 (*Hdac4*) in Mouse Embryonic Stem Cells

Russell C. Addis,[1] Megana K. Prasad,[2] Robert L. Yochem,[3] Xiangcan Zhan,[3] Timothy P. Sheets,[3] Joyce Axelman,[3] Ethan S. Patterson,[4] and Michael J. Shamblott[3*]

[1] *Department of Cell and Developmental Biology, and Institute for Regenerative Medicine, University of Pennsylvania, Philadelphia, Pennsylvania*

[2] *McKusick-Nathans Institute of Genetic Medicine, Johns Hopkins University School of Medicine, Baltimore, Maryland*

[3] *Department of Neurology, Johns Hopkins University School of Medicine and Hugo W. Moser Research Institute at the Kennedy Krieger Institute, Baltimore, Maryland*

[4] *Department of Developmental Biology, Washington University School of Medicine, St. Louis, Missouri*

ABSTRACT

OCT3/4 is a POU domain transcription factor that is critical for maintenance of pluripotency and self-renewal by embryonic stem (ES) cells and cells of the early mammalian embryo. It has been demonstrated to bind and regulate a number of genes, often in conjunction with the transcription factors SOX2 and NANOG. In an effort to further understand this regulatory network, chromatin immunoprecipitation was used to prepare a library of DNA segments specifically bound by OCT3/4 in undifferentiated mouse ES (mES) cell chromatin. One segment corresponds to a region within the first intron of the gene encoding histone deacetylase 4 (*Hdac4*), a Class II histone deacetylase. This region acts as a transcriptional repressor and contains at least two functional sites that are specifically bound by OCT3/4. HDAC4 is not expressed in the nuclei of OCT3/4+ mES cells and is upregulated upon differentiation. These findings demonstrate the participation of OCT3/4 in the repression of *Hdac4* in ES cells. J. Cell. Biochem. 111: 391–401, 2010.

KEY WORDS: EMBRYONIC STEM CELLS; OCT3/4; HDAC4; PLURIPOTENCY; TRANSCRIPTIONAL REGULATION

Embryonic stem (ES) cells are pluripotent cells derived from the inner cell mass of the mammalian blastocyst. ES cells and cells with ES-like properties have been derived from a number of mammalian species including mouse [Evans and Kaufman, 1981; Martin, 1981] and human [Thomson et al., 1998]. ES cells are capable of indefinite self-renewal in vitro and can differentiate into a wide variety of cell and tissue types, making them important tools for the study of development, cell differentiation, and gene function. Traditionally, mouse ES cells (mES) have been classified as pluripotent due to their ability, in chimeric animals, to form all tissues of the adult but failure to produce extraembryonic cell types of the trophectoderm and primitive endoderm lineages [Beddington and Robertson, 1989; Rossant, 2007]. This broad capacity to differentiate is also demonstrated by formation of embryoid bodies (EBs) in vitro and teratomas following transplantation into syngeneic or immunocompromised mice. The capacity of ES cells to participate so broadly in the differentiation of almost all of the specialized cell types of the body and retain indefinite capacity for self-renewal is both remarkable and rare. The list of cell types that share *most* of these properties includes embryonal carcinoma cells [Andrews et al., 1982; Andrews, 1984], embryonic germ cells [Resnick et al., 1992; Labosky et al., 1994; Shamblott et al., 1998] and, most recently, induced pluripotent stem (iPS) cells [Takahashi and Yamanaka, 2006; Okita et al., 2007; Yu et al., 2007].

Gene knockout studies have pointed to three factors, OCT3/4 [Nichols et al., 1998], SOX2 [Avilion et al., 2003], and NANOG [Chambers et al., 2003; Mitsui et al., 2003], that play essential roles in maintaining pluripotency in mouse embryos and ES cells. These factors have been shown to co-occupy promoter regions of hundreds of genes and to collectively maintain and regulate ES cell pluripotency [Boyer et al., 2005; Loh et al., 2006]. Identification of genes bound by OCT3/4 is a highly specific method to further understand how pluripotency is established and maintained in ES cells. OCT3/4 binding sites are often located in close proximity to SOX2 binding sites, but this is not always the case [Pesce and Scholer, 2001] and SOX2 is expressed in other tissues, frequently associated with stem or progenitor populations [Zappone et al., 2000; Muta et al., 2002; Ferri et al., 2004]. NANOG is specifically

*Correspondence to: Michael J. Shamblott, 707 North Broadway, Suite 518, Baltimore, MD 21205.
E-mail: shamblott@kennedykrieger.org
Received 28 January 2010; Accepted 12 May 2010 • DOI 10.1002/jcb.22707 • © 2010 Wiley-Liss, Inc.
Published online 19 May 2010 in Wiley Online Library (wileyonlinelibrary.com).

expressed in pluripotent cells, but has a less well-defined consensus binding site than OCT3/4. Among the most fully characterized genes for which both specific binding and regulation by OCT3/4 have been demonstrated are *fibroblast growth factor 4* (*Fgf4*) [Dailey et al., 1994], *Zpf42* (*Rex1*) [Ben-Shushan et al., 1998], *Fbx15* [Tokuzawa et al., 2003], *Utf1* [Nishimoto et al., 1999], Osteopontin (*Opn*) [Botquin et al., 1998], *Zpf206* [Wang et al., 2007], and *Zic3* [Lim et al., 2007] as well as *Pou5f1* (*Oct3/4*) [Okumura-Nakanishi et al., 2005], *Sox2* [Tomioka et al., 2002], and *Nanog* [Rodda et al., 2005] themselves.

Chromatin architecture is one means through which cells can globally and locally regulate gene expression. Covalent modifications to histones, such as the presence and absence of acetyl groups and methyl groups, can dramatically influence the access of transcription factors to regulatory regions. Several lines of evidence suggest that ES cells have regions of unique chromatin structure. In one study of mES chromatin, large regions of bivalent chromatin, having both repressive and activating histone methylation status, were identified and found to be more prevalent than in differentiated cell types. Approximately 50% of genes in these "bivalent" regions correspond to regions bound by OCT3/4, SOX2, and NANOG [Boyer et al., 2005]. Interestingly, areas identified as "bivalent" and predicted to be bound by OCT3/4, SOX2, and NANOG are more often transcriptionally silent [Bernstein et al., 2006], suggesting that repression is an important and common role for these factors. A second important finding in this area was that chromatin-binding proteins in mES cells are loosely associated with histone in ES cells and that histones H3 and H4 are both hyperacetylated in ES cells compared to differentiated cells [Meshorer et al., 2006]. This is in agreement with other findings that histones are deacetylated during ES cell differentiation and that differentiation is blocked by the histone deacetylase inhibitor trichostatin A [Lee et al., 2004]. These findings suggest that ES cells have regions of unique chromatin architecture, including hyperacetylated histones. It was also recently shown that nitric oxide treatment of mES cells leads to mesodermic differentiation via downregulation of OCT3/4 and upregulation of HDAC4 [Spallotta et al., 2010].

In this study, we sought to identify genes that are bound and regulated by OCT3/4. Here, we describe a regulatory region within an intron of the histone deacetylase 4 (*Hdac4*) gene that is bound by OCT3/4 and that acts as a repressor in reporter assays. We demonstrate that this repressive activity is reduced upon mutation of OCT3/4 binding sites and/or siRNA-mediated knockdown of *Oct3/4*. Furthermore, we show that OCT3/4 and HDAC4 are not colocalized in undifferentiated mES nuclei. Shortly after induction of mES cell differentiation, HDAC4 is expressed and localized in the cytoplasm. As differentiation proceeds, HDAC4 expression increases and is localized in the nuclei of a subset of cells. Together, these findings demonstrate that OCT3/4 directly regulates *Hdac4* transcription in mES cells.

MATERIALS AND METHODS

CHROMATIN IMMUNOPRECIPITATION

Chromatin was prepared [Weinmann et al., 2002; Wells and Farnham, 2002; Lavrrar and Farnham, 2004] from formaldehyde crosslinked mES cells (line ESD3) that were growing under optimal cell density conditions in the presence of exogenous leukemia inhibitory factor (LIF) and in contact with mitotically inactivated mouse embryo fibroblast (MEF) feeder layer using an anti-OCT3/4 antibody (C-20; Santa Cruz). Under these conditions, >95% of cells expressed OCT3/4 as judged by immunocytochemical staining. ChIP DNA was blunt-ended and ligated into the pZERO vector (Invitrogen). Colonies were picked at random and those with inserts >300 bp were DNA sequenced and compared to the mouse genome using the BLAT algorithm [Kent, 2002]. Predicted OCT3/4 and SOX2 binding sites were identified using the ESPsearch [Watt and Doyle, 2005] tool to generate pattern matching rules based on binding sites that have been demonstrated by EMSA to specifically bind OCT3/4 or SOX2. A graphical representation of the OCT3/4 consensus site position weight matrix was generated using WebLogo [Crooks et al., 2004].

ELECTROPHORETIC MOBILITY SHIFT ASSAYS

Nuclear extracts were prepared from ESD3 cells grown on MEFs by using the NE-PER extraction reagents (Pierce) and stored at −80°C. For EMSA, 3′-end biotinylated double-stranded DNA probes surrounding the predicted OCT3/4 binding sites were as follows, mutated bases are shown in lower case: O1, 5′-ACTGGATTTTAA-AGTTTGCAAATCAGGAGACAACCTAA-3′; O1mut, 5′-ACTGGATT-TTAAAGTggatctcgCAGGAGACAACCTAA-3′; O2, 5′-AAAGATAA-ATATGCTTCTAGCATTCTATCTCAAAAAAA-3′; O2mut, 5′-AAAG-ATAAATATGCTgacccgcgTCTATCTCAAAAAAA-3′; O3,5′-GATTA-CAATCAGTGTATGAGAATAGGGGAGATCCTAGG-3′; O3mut, 5′-GATTACAATCAGTGTcgacctcgAGGGGAGATCCTAGG-3′; O4, 5′-GCTCCCAAGCACTGCATGCCAGAAATTAATCAGGGGAG-3′; O4mut, 5′-GCTCCCAAGCACTGCcgaactgcAATTAATCAGGGGAG-3′; O56, 5′-GGAGACAACCTAAAGATGAGAAAGTTGGAATGTGAGAGATG-TAGCCTTTGCA-3′; O56mut, 5′-GGAGACAACCTAAAGcgtctacc-GTTGGAcgtgtatcGATGTAGCCTTTGCA-3′; O7, 5′-AATGCATATCT-AACTATTTACAACCAAGTCACATCAAA-3′; O7mut, 5′-AATGCA-TATCTAACTcgagctccCCAAGTCACATCAAA-3′; FGF4, 5′-TTTAAG-TATCCCATTAGCATCCAAACAAAGAGTTTTCTA-3′; FGF4mut, 5′-TTTAAGTATCCCcgccctcgCCAccacctAGTTTTCTA-3′. For DNA bind-ing reactions, 2.5 μl (∼15 μg) of nuclear extract was added to a 20 μl reaction containing 25–50 fmol biotinylated probe, 10 mM Tris pH 7.5, 50 mM KCl, 1 mM DTT, 2.5% glycerol, 5 mM $MgCl_2$, 100 ng/μl poly(dGdC) (Amersham Bioscience), and 0.05% Nonidet P-40. Unlabeled wild-type (WT) and mutant competitor probes were added in 50- to 200-fold molar excess. Binding reactions were resolved on pre-run 6% native polyacrylamide gels in 0.5× Tris–Borate–EDTA for 1 h at 100 V. DNA/protein complexes were transferred to nylon membrane and crosslinked using standard methods. Biotin-labeled complexes were detected by using LightShift® Chemiluminescent reagents (Pierce).

BINDING SITE PULLDOWN ASSAYS

For DNA binding reactions, 1.5 μg/μl mES cell nuclear extract, 1.3 μg/μl biotinylated double-strand probe, 10 mM Tris pH 7.5, 50 mM KCl, 1 mM DTT, 10% glycerol, 100 ng/μl poly(dGdC) (Amersham Bioscience) were incubated for 30 min at 25°C then incubated with streptavidin-coated agarose beads (Ultralink®,

Pierce) that had been preadsorbed in 1 μg/μl BSA, 100 ng/μl poly(dGdC), 100 ng/μl Herring sperm DNA. After washing, proteins were eluted from the beads by boiling in SDS gel loading buffer and were resolved on 8–20% gradient SDS–PAGE (Biorad), transferred to nylon membrane, blocked in 5% (w/v) dry milk in TBST (137 mM NaCl, 10 mM Tris, pH 7.4, 0.05% Tween-20) and sequentially incubated and detected with antibodies to OCT3/4 (BD Bioscience), SOX2 (Chemicon), NANOG (Chemicon), and isotype matched antibodies to non-binding proliferating cell nuclear antigen (PCNA) with overnight incubation in blocking buffer between antibodies. Both SOX2 and NANOG were detected in the final NANOG staining because both primary antibodies were raised in rabbit. Capture probes with mutated binding sites were used as a negative control and the OCT3/4 binding site within the Fgf4 gene was used as positive control.

LUCIFERASE REPORTER ASSAYS

mES cells (line ESD3) growing on mitotically inactivated MEFs were trypsinized and feeder layers reduced by serial 30 min incubations on plastic dishes. Approximately 1.9×10^5 mES cells per well of a 24-well plate were grown overnight in standard ES cell media supplemented with 1,000 U/ml LIF. Under these conditions >95% ES cells are OCT3/4+. Equimolar amounts of each firefly luciferase vector and the Renilla luciferase control vector were transiently transfected into triplicate wells of mES cells using Lipofectamine 2000 (Invitrogen) and ES cells were incubated for ~24 h. Luciferase assays were performed using the Stop-and-Glo Dual luciferase system (Promega). Values were normalized based on Renilla luciferase levels and reported as a fold change over minimal promoter (MP) ± standard error. Putative OCT3/4 regulatory regions were cloned into the pGL3 reporter system (Promega) with either the SV40 minimal promoter (SV40MP) or a synthetic MP [Edelman et al., 2000]. Regions were inserted in multiple orientations with respect to the promoter regions and DNA flanking the ChIP clone (B8F region) and were assayed in order to assess position and orientation dependence and provide experimental replication. Mutant luciferase reporter constructs were prepared by introduction of novel restriction sites into the O1 and O3 binding sites of the B8F region placed upstream of the SV40MP. Primers were as follows, mutated bases shown in lower case: O1m, 5′-GCTATTATCCCTTTCT-CAAGAACTGGATTTTAAAGTTTcgaTcgCAGGAGACAACCTAAAG-ATGAGAA-3′; O3m, 5′-GGTCCTTGATTACAATCAGTGTGTATGctt-AgGGGAGATCCTAGGACCAAGAA-3′.

OCT3/4 KNOCKDOWN

OCT3/4 expression level was reduced in mES cells by lipofection of three siRNA duplexes (Invitrogen Stealth RNAi) that have been demonstrated to reduce *Oct3/4* mRNA and protein levels in mES cells [Hough et al., 2006]. The sense strand sequences of these constructs were: S5, 5′-CCAAUGCCGUGAAGUUGGAGAAGGU-3′; S6, 5′-CCCGGAAGAGAAAGCGAACUAGCAU-3′; S7, 5′-CCAAU-CAGCUUGGGCUAGAGAAGGA-3′. An siRNA duplex consisting of scrambled S6 sequence was used as a negative control: SCR, 5′-GGAGAGAAACCACGCGCACAUUAGA-3′. mES cells were lipofected with siRNA constructs using Lipofectamine RNAiMAX (Invitrogen) according to the manufacturer's protocol for reverse transfection. Cells were plated without feeders at a density of 40,000 cells/cm^2 with a final siRNA concentration of 50 nM, then incubated for 24 h prior to lipofection of luciferase vectors using Lipofectamine 2000. After an additional 24 h, protein was collected from mES cells treated with either Lipofectamine RNAiMAX alone, or in combination with each of the four siRNA constructs. Western blot was stained serially with antibodies recognizing OCT3/4 (BD Biosciences) and PCNA (Santa Cruz Biotechnology).

ES CELL DIFFERENTIATION, RNA PREPARATION, IMMUNOCYTOCHEMISTRY, AND WESTERN BLOTTING

To initiate mES cell differentiation, mES cells were plated serially two times for a total of 1 h on adherent plastic dishes to reduce MEF cell contamination. mES cells were then counted and resuspended in media without LIF at 1,000 cells per 20 μl drop and placed on the lid of a tissue culture dish and incubated for 2 days to form EBs. After this, EBs were placed into non-adherent plastic dishes for an additional 3 days (EB days 3–5) then plated onto adherent gelatin-coated plastic dishes and glass cover slips. EBs were removed at intervals (EB 6–10 and 13) and a 50% media replacement was carried out on EB7. RNA was prepared from MEF-reduced mES cells, adherent EBs, and MEFs by using the Qiagen RNA miniprep kit. mES cells that were plated at ~1.5×10^4 cells/cm^2 on glass chamber slides that had been previously plated with mitotically inactivated MEFs then grown for 24 h in the presence of LIF, mES cells that were plated at similar density on gelatin-coated glass cover slips for 72 h in the presence of LIF and adherent EBs were fixed in 4% paraformaldehyde, blocked in 5% donkey serum, 1% (w/v) bovine serum albumin, 0.3% Triton X-100 prepared in PBS and stained with antibodies to OCT3/4 (BD Biosciences), or HDAC4 (Upstate). Detection was done with fluorescently labeled secondary antibodies (Molecular Probes). Confocal microscopy analysis was performed on mES cells grown on cover slips and adherent EBs. Cell counting was carried out on five to eight randomly selected fields and counting >1,000 nuclei per time point. For Western blots, 10 μg nuclear and cytoplasmic protein extract prepared from mES cells, and cells at EB6, 8, 10, and 13 were resolved on 12% PAGE, electrophoretically transferred to PVDF membranes and incubated with anti-HDAC4 antibody. The membrane was post-stained with 0.1% (w/v) Ponceau S in 5% acetic acid to ensure equal protein loading and transfer.

QUANTITATIVE REVERSE TRANSCRIPTASE–POLYMERASE CHAIN REACTIONS

Synthesis of cDNA was performed by using oligo (dT) primers in a standard Moloney Murine Leukemia Virus reaction carried out at 42°C. Quantitative PCR was carried out using SYBR green or Taqman chemistry (Applied Biosystems) on three independently prepared RNA samples of each cell type, with at least four replicate readings of each sample. mRNA expression levels of *Oct3/4* and *Hdac4* were normalized by mRNA levels of *Gapdh*. Additionally, the identities of all amplimers were confirmed by DNA sequencing following standard PCR reactions. Primers were as follows: OCT3/4-N, 5′-AGAGGGAACCTCCTCTGAGC-3′; OCT3/4-C, 5′-AGATGGTGGTCT-GGCTGAAC-3′; HDAC4N, 5′-CAGACAGCAAGCCCTCCTAC-3′; HDAC4C, 5′-AGACCTGTGGTGAACCTTGG-3′; GAPDHN, 5′-GGC-AAATTCAACGGCACAGT-3′; GAPDHC, 5′-AGATGGTGATGGGC-

TTCCC-3′. Taqman primer/probe sets were Mm01299557_m1 (*Hdac4*), 4352932 (*Gapdh*).

EXPRESSION OF MUTANT HDAC4 CONSTRUCTS

Fusion proteins consisting of mouse HDAC4 with three amino acid substitutions (S246A/S467A/S632A) that block cytoplasmic shuttling and either enhanced green fluorescent protein (EGFP) (EGFP–HDAC4–TM1) or the FLAG epitope (FLAG–HDAC4–TM1) [Wang and Yang, 2001] and EGFP alone were expressed in mES cells under the control of the cytomegalovirus (CMV) promoter by lipofection using Lipofectamine 2000 (Invitrogen) in triplicate. Twenty-four and 48 h after transfection, cells were trypsinized, counted, and cells were immobilized on glass slides by using a cytospin. Cells were fixed in 2% paraformaldehyde for 5 min, blocked and stained for expression of OCT3/4. EGFP expression was detected by using an anti-GFP antibody conjugated to Alexa488 (Invitrogen). The FLAG epitope was detected by anti-FLAG antibody (Sigma). Greater than 1,000 nuclei were examined at each time point.

RESULTS

LIBRARY SCREENING, VALIDATION, AND DETERMINATION OF OCT3/4 CONSENSUS BINDING SITE

A ChIP library prepared from formaldehyde crosslinked mES cell chromatin immunoprecipitated with an antibody to OCT3/4 was screened by random clone selection. Forty-three of the 84 clones (51%) were unambiguously matched to non-repetitive mouse loci using the BLAT genome alignment tool [Kent, 2002]. Remaining clones were either substantially repetitive or ambiguous matches (37%) or failed sequencing (12%). Twenty-six of the 43 remaining clones (60%) were prioritized for further analysis because they contained a match to the consensus OCT3/4 binding sequences and were within a gene or less than 10 kb from a gene. Two OCT3/4 consensus binding sequences were determined by comparing OCT3/4 binding sites in *Fgf4* [Dailey et al., 1994], *Rex1* [Ben-Shushan et al., 1998], *Fbx15* [Tokuzawa et al., 2003], *Utf1* [Nishimoto et al., 1999], *Opn* [Botquin et al., 1998], and *Nanog* [Kuroda et al., 2005] genes (Fig. 1A).

CHARACTERIZATION OF A PUTATIVE OCT3/4 REGULATORY REGION IN THE *HDAC4* GENE

One of the 26 clones identified in our library screening was a 734 bp fragment within the first intron of the *Hdac4* gene (termed B8 region here, nucleotide 382–1,116 in Fig. 1B). Within this fragment, we identified six predicted OCT3/4 binding sites and one predicted SOX2 binding site that was >70 bp from the nearest OCT3/4 site. We also identified a larger ~1.6 kb fragment with DNA flanking the B8 region (B8F) containing one additional predicted OCT3/4 binding site and two additional predicted SOX2 binding sites that are >100 bp from any predicted OCT3/4 binding site (Fig. 1B). We performed electrophoretic mobility shift assays (EMSA) by incubating biotinylated double-strand probes surrounding these predicted OCT3/4 binding sites with mES cell nuclear extract. Binding specificity was determined by competition with excess WT unlabeled probes and failure to compete by excess of probes with mutated OCT3/4 binding sites (MUT). Of the seven sites examined, only two showed binding of ES cell nuclear extract. The O1 site probe demonstrated clean and specific binding (Fig. 2A), while the O3 site was somewhat less effectively bound or thoroughly competed away by unlabeled WT probe (Fig. 2B). All the remaining predicted OCT3/4 binding sites failed to demonstrate specific binding (data not shown). None of the sites demonstrated specific binding in the presence of MEF cell nuclear extract (data not shown). Biotinylated double-stranded DNA probes flanking the O1 and O3 sites were used to pull down proteins in mES cell nuclear extract that bound these sites. An OCT3/4 binding site within the *Fgf4* gene was used as a positive control and the mutated O1 putative binding site was used as a negative control. As shown in Figure 2C, the O1, O3, and *Fgf4* gene sites all bound OCT3/4, SOX2, and NANOG. These results establish that OCT3/4 can bind these sites and suggest that OCT3/4 binds as a complex with SOX2 and NANOG, since none of the capture probes contain consensus SOX2 or NANOG binding sites.

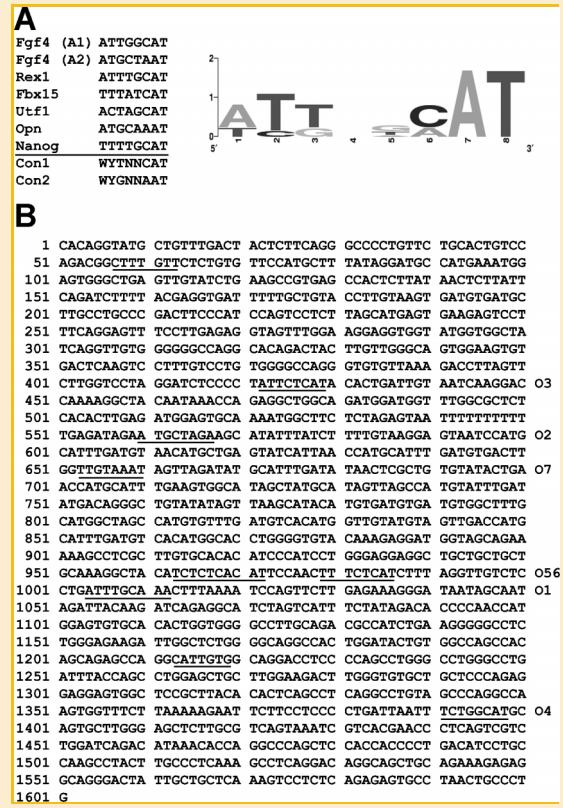

Fig. 1. A: Two consensus OCT3/4 binding sequences (Con1 and Con2) derived from alignment of seven OCT3/4 binding regions. W:A,T; Y:C,T; N:A,T,G,C. The graphical representation of a position weight matrix was generated using WebLogo (http://www.weblogo.berkeley.edu). B: B8 flanking region with predicted OCT3/4 and SOX2 binding sites (underlined). OCT3/4 sites are shown at right. B8 region is from 382 to 1,115 bp.

REPRESSOR ACTIVITY OF OCT3/4 REGULATORY REGION

To determine the impact of the putative OCT3/4 binding region on transcription, we performed luciferase reporter assays using a series of vectors containing a synthetic MP [Edelman et al., 2000] or SV40MP and the B8 and B8F regions placed in the same orientation

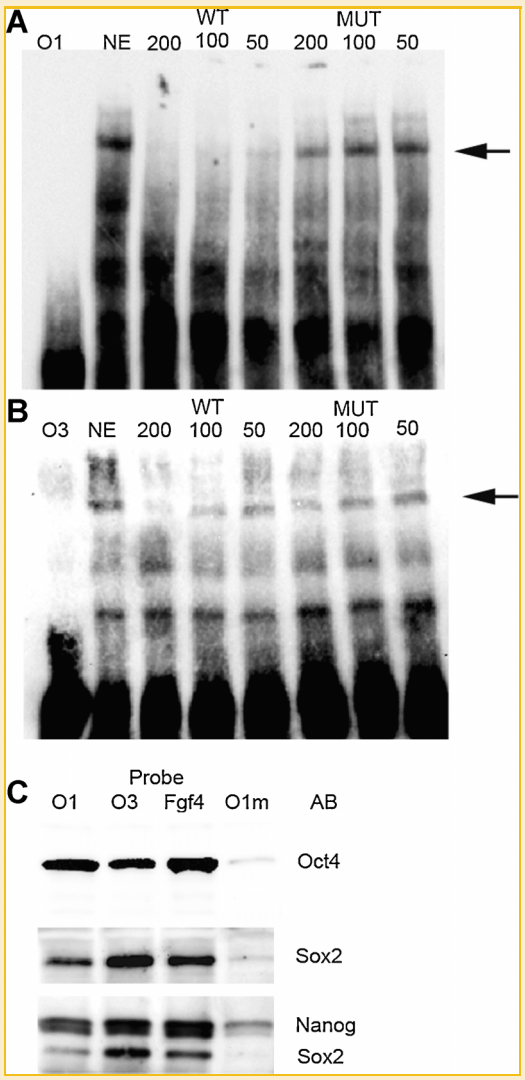

Fig. 2. Binding specificity of the *Hdac4* O1 and O3 regions. A,B: EMSA results. Lanes O1/O3, labeled probe only; NE, probe with nuclear extract; WT, molar excess unlabeled wild-type probe; MUT, molar excess unlabeled mutated probe. Arrows at right indicate shifted complex. C: Western blot detection of proteins pulled down by probes as indicated. Antibodies to NANOG and SOX2 were both detected by the secondary antibody and were distinguished by mass.

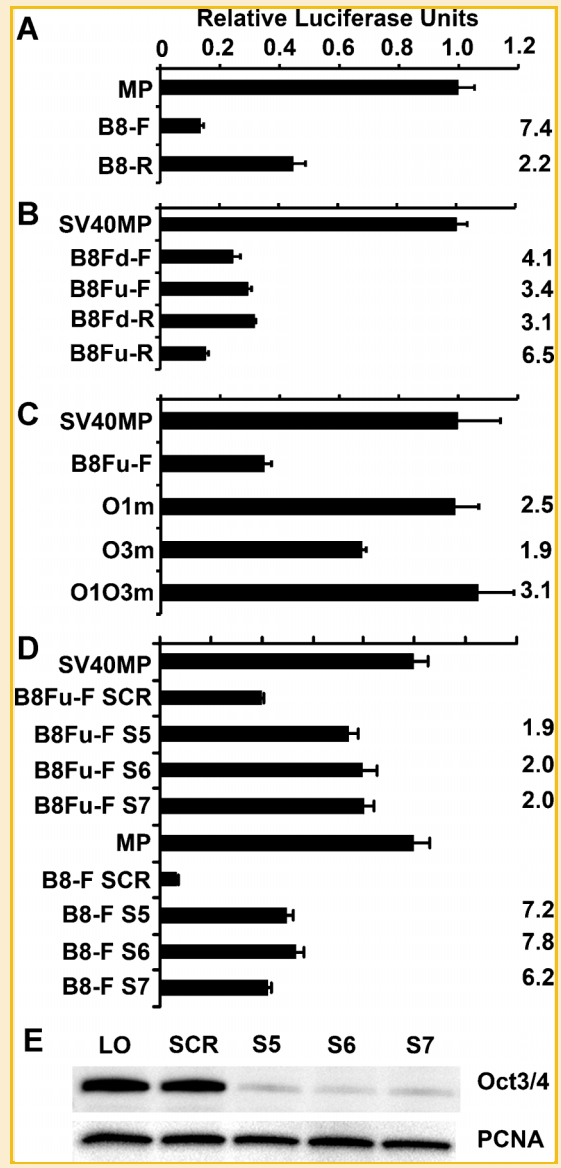

Fig. 3. Effects of the *Hdac4* putative OCT3/4 binding region on transcription of minimal promoters in mES cells. Minimal promoter activity set at 1 U. MP, synthetic minimal promoter; SV40MP, SV40 minimal promoter; B8-F, B8 region in the forward orientation; B8-R, B8 region in the reverse orientation; B8Fd-F, B8 flank region in the forward orientation downstream of SV40MP; B8Fu-F, B8 flank region in the forward orientation upstream of SV40MP; B8Fd-R, B8 flank region in the reverse orientation downstream of SV40MP; B8Fu-R, B8 flank region in the reverse orientation upstream of SV40MP. A: Fold decrease in luciferase compared to MP indicated to the right. B: Fold decrease in luciferase compared to SV40MP indicated to the right. C: O1m, B8Fu-F with mutation in O1 binding site; O3m, B8Fu-F with mutation in O3 binding site; O1O3m, B8Fu-F with mutation in O1 and O3 binding sites. Fold increase in luciferase compared to B8Fu-F indicated to the right. D: Impact of treatment with OCT3/4 siRNA constructs S5, S6, S7, and SCR (scrambled S6 sequence, negative control) shown below B8Fu-F and B8-F. Fold increase in luciferase compared to B8Fu-F SCR and B8-F SCR indicated to the right. E: Western blot analysis of the effect of OCT3/4 siRNAs on OCT3/4 and proliferating cell nuclear antigen (PCNA) protein levels. LO, treated with Lipofectamine RNAiMAX alone; SCR, S5, S6, S7, treated with siRNA constructs.

they were with respect to transcription of the *Hdac4* gene (-F) and in reverse orientation (-R). The B8F region was also placed upstream (u) of the MP/luciferase and downstream (d). Every combination tested resulted in a statistically significant ($P < 0.001$) repression of MP transcription in undifferentiated mES cells (Fig. 3A,B). The mean level of transcriptional repression among B8 and B8F constructs is approximately fourfold and there is no evidence that the flanking region included in B8F confers additional transcriptional repression. The B8Fu-F and B8-F constructs were tested in mES cells both with and without feeder layers and there was no significant difference between the results (data not shown).

Mutating the O1 and O3 sites had a statistically significantly effect ($P < 0.001$) of relieving transcriptional repression by 2.5- and 1.9-fold, respectively, as compared to the WT B8F region. The effect

of mutating both sites resulted in a statistically significant ($P < 0.001$) threefold increase in transcriptional activity, which fully reversed the repressive effect of the B8F region (Fig. 3C).

The effect of reducing OCT3/4 levels on B8F transcriptional regulation was investigated by transient transfection of three siRNA duplexes targeted to different sites of the *Oct3/4* gene. All three siRNAs reduced OCT3/4 protein levels by greater than 50% approximately 48 h after transfection (Fig. 3E), consistent with the timing and reduction of protein levels observed for siRNA S6 [Hough et al., 2006]. Reduction in OCT3/4 protein levels corresponded to statistically significant ($P < 0.001$) 1.9- to 8-fold decreases in the repressive effects of both the B8 and B8F regions and returned expression levels to $48.7 \pm 5.5\%$ and $77.9 \pm 3.4\%$ of MP activity, respectively (Fig. 3D). However, in this experiment there was no significant difference seen in *Hdac4* mRNA expression levels. This finding was replicated in subsequent experiments plating mES on human fibroblast feeder layer to reduce feeder layer-derived *Hdac4* expression and on a second mES cell line (data not shown).

HDAC4 AND *OCT3/4* MRNA EXPRESSION DURING MES CELL DIFFERENTIATION

To determine the expression levels of *Oct3/4* and *Hdac4* mRNA in mES cells, we grew mES cells on MEF feeder layers in the presence of exogenous LIF and then harvested EBs over a 13-day period starting at day 6 (EB6). This initial time point is 24 h after EB attachment and when strong expression of *Hdac4* was first observed in the nucleus of differentiating mES cells. As shown in Figure 4A, *Oct3/4* mRNA levels decreased significantly by EB6 (28.6-fold, $P < 0.01$) compared to undifferentiated mES cells. *Hdac4* mRNA levels decreased significantly between mES cells and EB6 (2.9-fold, $P < 0.001$) then increased with respect to mES cells on EB7 (6.2-fold, $P < 0.05$), EB8 (2.4-fold, $P < 0.001$), EB9 (5.6-fold, $P < 0.001$), EB10 (5.7-fold, $P < 0.01$), and EB13 (8.0-fold, $P < 0.001$). MEFs expressed no detectable *Oct3/4* and less *Hdac4* mRNA than mES cells (1.7-fold, $P < 0.05$).

OCT3/4 AND HDAC4 PROTEIN EXPRESSION DURING MES CELL DIFFERENTIATION

Class IIa HDACs such as HDAC4 are known to shuttle between the cytoplasm, where they are inactive with respect to histone deacetylation and transcriptional repression and the nucleus [Cress and Seto, 2000; Grozinger and Schreiber, 2000]. As seen in Figure 4B, low levels of HDAC4 can be detected in the nuclei and cytoplasm of mES cell cultures that have been depleted of contaminating MEFs. By EB6, HDAC4 is expressed at high levels in the nucleus and to a lesser extent in the cytoplasm of differentiating cells. To understand the relationship between HDAC4 and OCT3/4 expression, we examined undifferentiated and differentiating mES cells using immunocytochemistry. We were unable to find a single nucleus that costained for OCT3/4 and HDAC4 in >2,000 nuclei examined in ~250 mES cell colonies. Many examples of OCT3/4−, nuclear HDAC4+ cells were observed within and in close proximity to ES colonies (Fig. 5A–F). Some of these cells, such as the large HDAC4+ nuclei seen in Figure 5A, are MEFs, a finding confirmed by staining MEFs alone. When mES cells

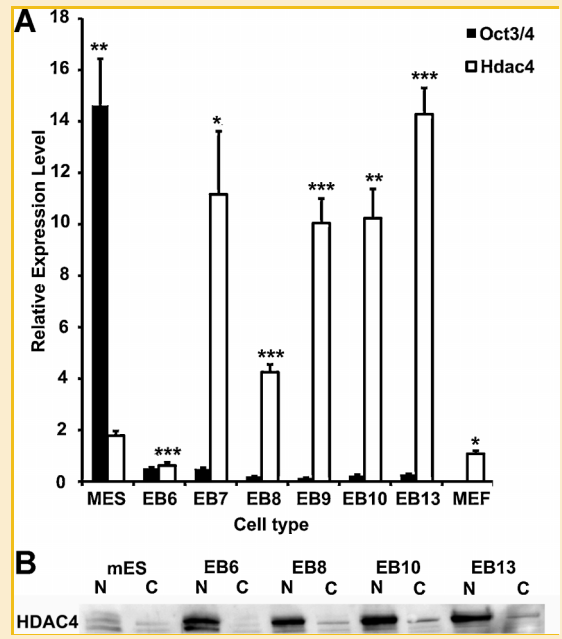

Fig. 4. Expression level of *Oct3/4* and *Hdac4* following mES cell differentiation. A: Mean mRNA expression level (n = 3) of *Oct3/4* (black) and *Hdac4* (white) and normalized to the level of *Gapdh* mRNA shown on Y-axis. Cell type shown on X-axis, mES, undifferentiated mES cells; EB6–13, embryoid bodies (EB) after 6–13 days differentiation; MEF, mouse embryo fibroblasts. Significant difference compared to levels in mES cells determined by Student's *t*-test. $^{*}P < 0.05$; $^{**}P < 0.01$; $^{***}P < 0.001$. B: Western blot of HDAC4 protein expression in undifferentiated mES cells (mES) and at EB days 6, 8,10, 13. N, nuclear extract; C, cytoplasmic extract.

were grown under ideal circumstances (on a confluent MEF feeder layer in the presence of exogenous LIF and in small colonies) OCT3/4+ cells were largely HDAC4−. When mES cells were grown in suboptimal conditions; in the absence of MEF feeder cells, for prolonged periods between disaggregation or in very large colonies, mES cells began to differentiate and migrate away from the colony. Differentiated colonies contained cells expressing OCT3/4 at different levels and OCT3/4 expression level was inversely correlated to HDAC4 expression level. As seen in Figure 5G–I, a 1-μm focal plane of a differentiating mES cell colony contains cells expressing high levels of OCT3/4 and little or no HDAC4, weakly OCT3/4+ and cytoplasmic HDAC4 positive cells, and OCT3/4− and nuclear HDAC4+ cells. Subsequent experiments consistently demonstrated that differentiating weakly OCT3/4 positive cells begin to express cytoplasmic HDAC4.

Throughout the EB differentiation time course, OCT3/4+ cells were present within colonies. On EB6 low levels of HDAC4 can be seen in the cytoplasm of cells within colonies, with the highest levels in cells that are OCT3/4 negative (Fig. 6A–F). HDAC4 is located in the nucleus of approximately 0.8% (11/1,354) of OCT3/4 negative cells on the periphery of colonies (arrowhead in Fig. 6F). The HDAC4 expression pattern on EB7 (Fig. 6G–L) is similar to that observed on EB6 except that levels in the cytoplasm appeared to be higher than levels on EB6 and the level and frequency (10%, 108/1,075) of nuclear localization were also

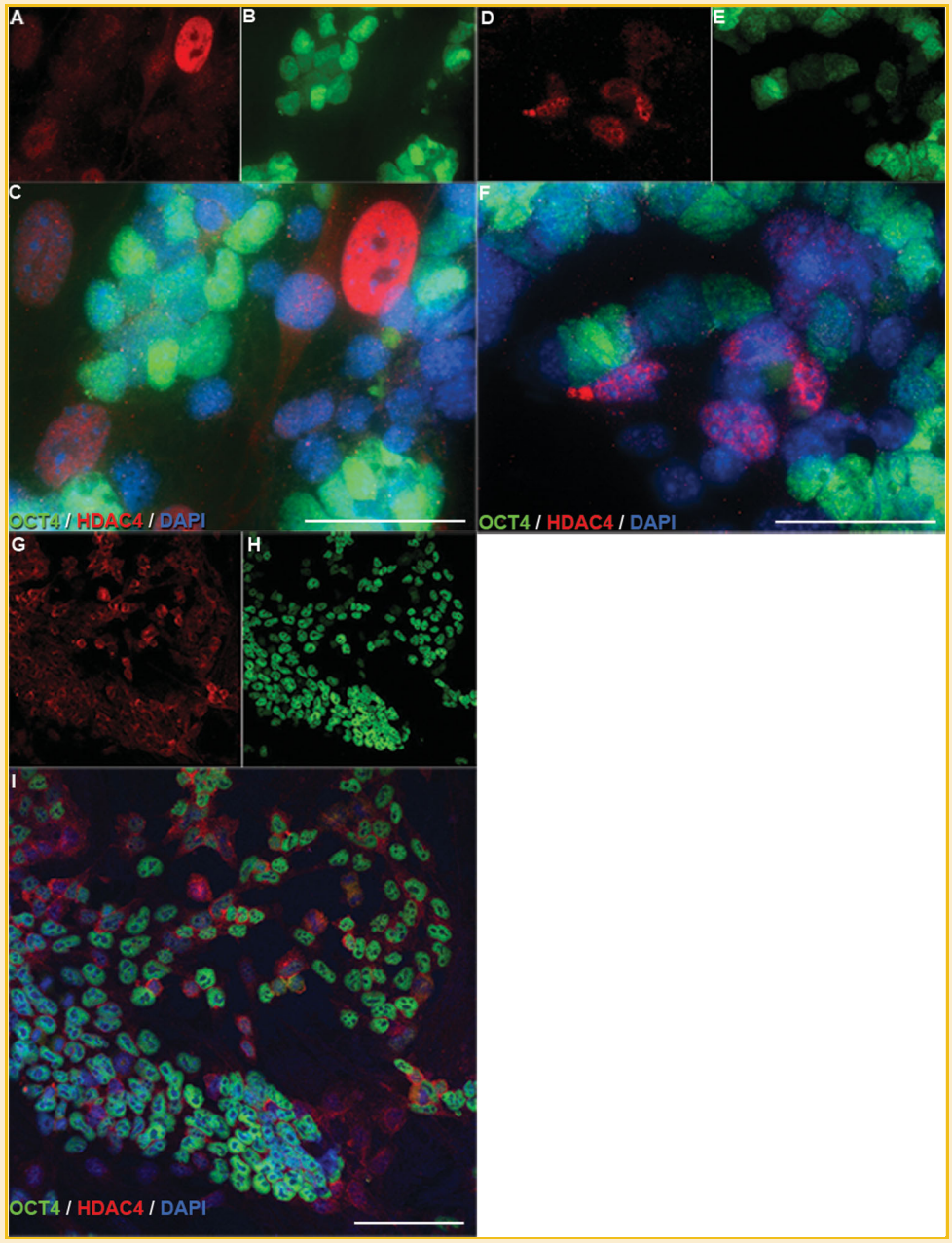

Fig. 5. Expression of OCT3/4 and HDAC4 in differentiating mES cells. A–F: mES cells growing on MEF feeder layer for 24 h. G–I: 1-μm focal plane of mES cells growing on gelatin-coated glass coverslips for 72 h. B,E,H: OCT3/4; A,D,G: HDAC4;. Scale bars: C,F: 50 μm, I: 100 μm.

increased. Between EB8-13, HDAC4 is expressed and localized at high levels in the nucleus of OCT3/4− cells and in the cytoplasm of cells weakly expressing OCT3/4 and OCT3/4 negative cells. The percentage of HDAC4+ cells on EB8 and 9 were 22% (271/1,230) and 42% (973/2,295), respectively. The high-cell density on EB10 and EB13 prohibited determination of HDAC4 expression frequency. At each time point, nuclear HDAC4+ cells were distributed heterogeneously in patches, resulting in high-cell count variability. However, the expression pattern evident from immunocytochemical staining is consistent with the Western blot analysis (Fig. 4B).

COLOCALIZATION OF HDAC4 AND OCT3/4

Since no evidence of OCT3/4 and HDAC4 colocalization was detected in mES cell nuclei under normal circumstances, we investigated the effects of constitutive nuclear HDAC4 expression on OCT3/4+ mES cells. WT HDAC4 has intrinsic nuclear import and export signals [Wang and Yang, 2001]. A combination of three single amino acid substitutions (S246A/S467A/S632A) in the N-terminus of HDAC4 (HDAC4–TM1) entirely blocks binding to 14-3-3 protein and subsequent cytoplasmic shuttling [Grozinger and Schreiber, 2000; Wang et al., 2000]. As shown in Table I, 24 h after transient transfection of an EGFP–HDAC4–TM1 fusion protein

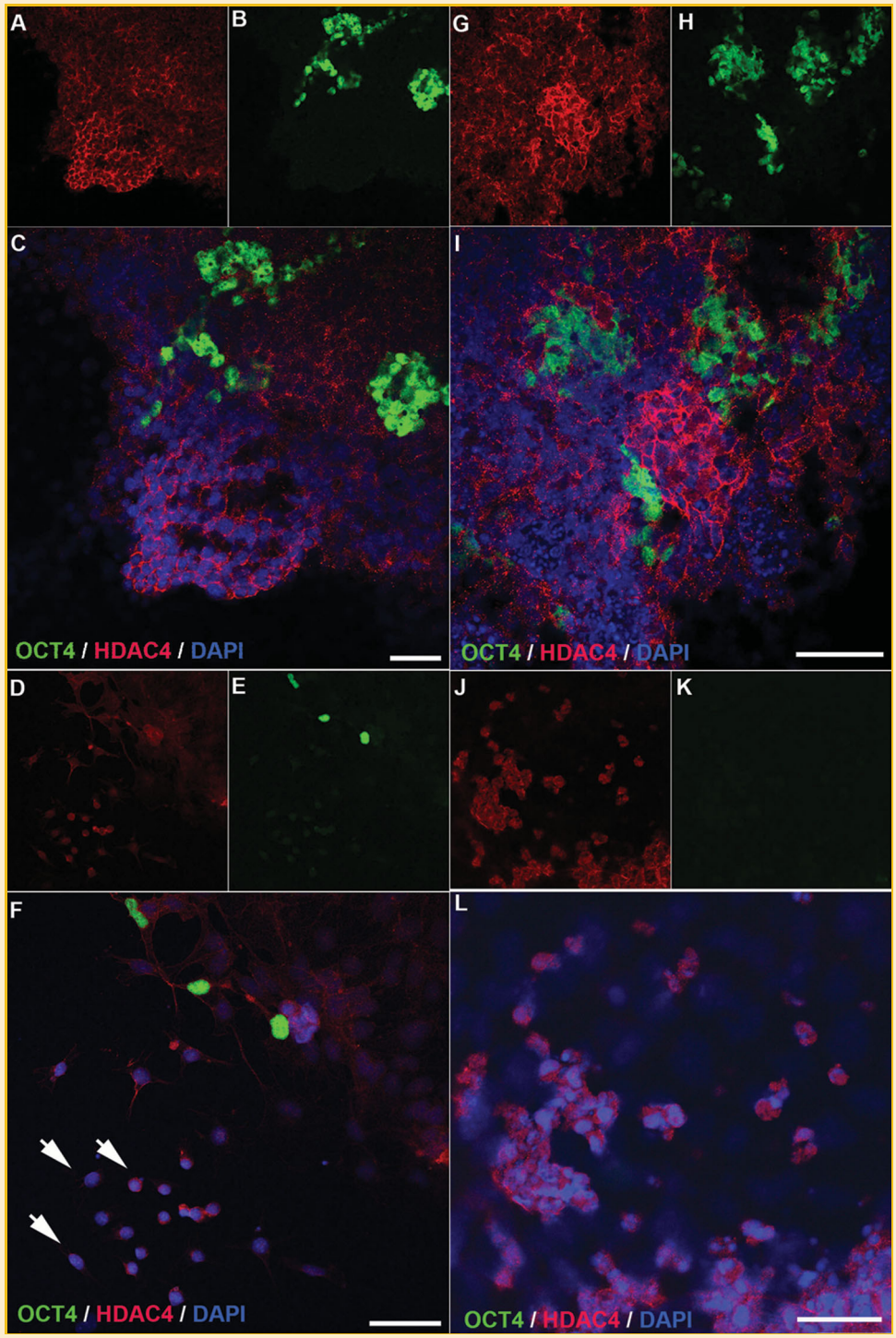

Fig. 6. Expression of OCT3/4 and HDAC4 in differentiated mES cells on EB day 6 (A–F), EB day 7 (G–L). B,E,H,K: OCT3/4; A,D,G,K: HDAC4. Examples of OCT3/4− nuclear HDAC4+ cells marked by arrowheads in F. 1-μm focal plane, Scale bar: 50 μm.

under the control of the CMV promoter in mES cells, 93 ± 5% of cells were OCT3/4+ and 67 ± 4% were EGFP–HDAC4–TM1+. EGFP–HDAC4–TM1 was localized in the nucleus of virtually all cells in which it was detected. Of the EGFP–HDAC4–TM1+ cells, 89 ± 6% were OCT3/4+. After 48 h, 80 ± 6% of cells were OCT3/4+ but only 2 ± 0.6% were EGFP–HDAC4–TM1+, an approximately 33-fold decrease in the percentage of EGFP–HDAC4–TM1 expressing cells. Likewise, 1.3 ± 0.9% of OCT3/4+ cells expressed EGFP–HDAC4–TM1+, an approximately 68-fold decrease in the percentage of OCT3/4+ cells expressing EGFP–HDAC4–TM1. Transient transfection with EGFP alone driven by the CMV promoter resulted in approximately 40% of cells expressing EGFP after 24 h and

TABLE I. Incompatibility of Nuclear HDAC4 and OCT3/4 in Mouse Embryonic Stem Cells

	HDAC4–TM1		OCT3/4		HDAC4–TM1+ OCT3/4	
Hours post-transfection	Positive/total	%	Positive/total	%	Positive/total	%
24	722/1,078	67 ± 4.0	1,002/1,078	93 ± 5.0	642/1,078	60 ± 4.0
48	23/1,191	2 ± 0.6	952/1,191	80 ± 6.0	16/1,191	1.3 ± 0.9

approximately 50% after 48 h with no decrease in the percentage of EGFP/OCT3/4 coexpression. The loss of EGFP–HDAC4–TM1+ cells was not due to the presence of EGFP in the mES cell nuclei, as a similar drop in the percentage of FLAG–HDAC4–TM1 cells was observed. This finding was reproduced two additional times with similar results. Attempts to generate stable mES lines expressing EGFP–HDAC4–TM1 or FLAG epitope–HDAC4–TM1 fusion proteins by cotransfection with a vector expressing a hygromycin resistance gene failed repeatedly. However, stable lines of 293T cells expressing both fusion proteins were routinely isolated using these vectors, as were stable lines of mES cells expressing EGFP under the control of the CMV promoter. These results suggest that nuclear HDAC4 is not compatible with OCT3/4 in mES cells.

DISCUSSION

We have identified a regulatory region within the first intron of the *Hdac4* gene. This region, which we have termed B8F, functions as a transcriptional repressor in mES cells and contains at least two sites that specifically bind OCT3/4 in complex with SOX2 and NANOG. Mutation of these sites and/or knockdown of *Oct3/4* expression is sufficient to reverse the repressive activity of B8F. Consistent with this regulatory role, OCT3/4 and HDAC4 are not colocalized in the nuclei of undifferentiated ES cells. Failed attempts to transiently and stably express a mutant form of HDAC4 that cannot be exported from the nucleus suggest that localization of HDAC4 in the nuclei of mES cells is not compatible with continued expression of OCT3/4 or long-term survival of mES cells.

As OCT3/4 expression levels decrease during mES cell differentiation, coexpression of OCT3/4, and cytoplasmic HDAC4 can be detected. This occurs in cells within mES colonies and is increased under conditions that are unfavorable for long-term maintenance, such as in the absence of MEF feeder layer cells. This suggests a scenario in which OCT3/4 does not fully repress *Hdac4* gene expression, due either to a decrease in OCT3/4 below a threshold level or a counteracting induction. It is possible that such cells require some amount of HDAC4 for further differentiation. *Hdac4* transcription and both nuclear and cytoplasmic HDAC4 levels increase by day 7 of EB formation as compared to mES cells, and remain high throughout the 13-day differentiation time course.

Our study is the first to implicate OCT3/4 in the regulation of *Hdac4*. Since the B8F regulatory sequence is located more than 15 kb downstream from the *Hdac4* transcriptional start site, it could not have been identified in "ChIP-on-chip" studies that examined regions more proximal to gene promoters [Boyer et al., 2005; Loh et al., 2006]. The fact that *Oct3/4* knockdown in mES cells did not lead to a significant increase in *Hdac4* expression indicates that OCT3/4-*Hdac4* regulation is not a simple binary system. It is likely that other factors, in addition to OCT3/4, contribute to *Hdac4* repression in mES cells. Likewise, it is reasonable to assume that more is required to activate *Hdac4* transcription than the removal of OCT3/4. The B8F regulatory element, located in the first intron of *Hdac4,* may act in concert with the *Hdac4* promoter, other transcriptional regulatory elements and cellular localization machinery to appropriately modulate the histone acetylation state of a subset of genes. The contribution of OCT3/4 to the transcriptional repression of *Hdac4* is consistent with previous findings indicating that the chromatin of ES cells is hyperacetylated, and that ES cell differentiation requires histone deacetylation. Future studies will determine the degree to which HDAC4 directly contributes to this deacetylation. The present study demonstrates yet another example in the ever-growing list of critical roles played by OCT3/4 in maintaining pluripotency.

ACKNOWLEDGMENTS

We would like to thank Dr. Xiang-Jiao Yang (McGill University Health Center) for the EGFP and FLAG–HDAC4–TM1 expression vectors.

REFERENCES

Andrews PW. 1984. Retinoic acid induces neuronal differentiation of a cloned human embryonal carcinoma cell line in vitro. Dev Biol 103:285–293.

Andrews PW, Goodfellow PN, Shevinsky LH, Bronson DL, Knowles BB. 1982. Cell-surface antigens of a clonal human embryonal carcinoma cell line: Morphological and antigenic differentiation in culture. Int J Cancer 29:523–531.

Avilion AA, Nicolis SK, Pevny LH, Perez L, Vivian N, Lovell-Badge R. 2003. Multipotent cell lineages in early mouse development depend on SOX2 function. Genes Dev 17:126–140.

Beddington RS, Robertson EJ. 1989. An assessment of the developmental potential of embryonic stem cells in the midgestation mouse embryo. Development 105:733–737.

Ben-Shushan E, Thompson JR, Gudas LJ, Bergman Y. 1998. Rex-1, a gene encoding a transcription factor expressed in the early embryo, is regulated via Oct-3/4 and Oct-6 binding to an octamer site and a novel protein, Rox-1, binding to an adjacent site. Mol Cell Biol 18:1866–1878.

Bernstein BE, Mikkelsen TS, Xie X, Kamal M, Huebert DJ, Cuff J, Fry B, Meissner A, Wernig M, Plath K, Jaenisch R, Wagschal A, Feil R, Schreiber SL, Lander ES. 2006. A bivalent chromatin structure marks key developmental genes in embryonic stem cells. Cell 125:315–326.

Botquin V, Hess H, Fuhrmann G, Anastassiadis C, Gross MK, Vriend G, Scholer HR. 1998. New POU dimer configuration mediates antagonistic control of an osteopontin preimplantation enhancer by Oct-4 and Sox-2. Genes Dev 12:2073–2090.

Boyer LA, Lee TI, Cole MF, Johnstone SE, Levine SS, Zucker JP, Guenther MG, Kumar RM, Murray HL, Jenner RG, Gifford DK, Melton DA, Jaenisch R, Young RA. 2005. Core transcriptional regulatory circuitry in human embryonic stem cells. Cell 122:947–956.

Chambers I, Colby D, Robertson M, Nichols J, Lee S, Tweedie S, Smith A. 2003. Functional expression cloning of Nanog, a pluripotency sustaining factor in embryonic stem cells. Cell 113:643–655.

Cress WD, Seto E. 2000. Histone deacetylases, transcriptional control, and cancer. J Cell Physiol 184:1–16.

Crooks GE, Hon G, Chandonia JM, Brenner SE. 2004. WebLogo: A sequence logo generator. Genome Res 14:1188–1190.

Dailey L, Yuan H, Basilico C. 1994. Interaction between a novel F9-specific factor and octamer-binding proteins is required for cell-type-restricted activity of the fibroblast growth factor 4 enhancer. Mol Cell Biol 14: 7758–7769.

Edelman GM, Meech R, Owens GC, Jones FS. 2000. Synthetic promoter elements obtained by nucleotide sequence variation and selection for activity. Proc Natl Acad Sci USA 97:3038–3043.

Evans MJ, Kaufman MH. 1981. Establishment in culture of pluripotential cells from mouse embryos. Nature 292:154–156.

Ferri AL, Cavallaro M, Braida D, Di Cristofano A, Canta A, Vezzani A, Ottolenghi S, Pandolfı PP, Sala M, DeBiasi S, Nicolis SK. 2004. Sox2 deficiency causes neurodegeneration and impaired neurogenesis in the adult mouse brain. Development 131:3805–3819.

Grozinger CM, Schreiber SL. 2000. Regulation of histone deacetylase 4 and 5 and transcriptional activity by 14-3-3-dependent cellular localization. Proc Natl Acad Sci USA 97:7835–7840.

Hough SR, Clements I, Welch PJ, Wiederholt KA. 2006. Differentiation of mouse embryonic stem cells after RNA interference-mediated silencing of OCT4 and Nanog. Stem Cells 24:1467–1475.

Kent WJ. 2002. BLAT-the BLAST-like alignment tool. Genome Res 12:656–664.

Kuroda T, Tada M, Kubota H, Kimura H, Hatano SY, Suemori H, Nakatsuji N, Tada T. 2005. Octamer and Sox elements are required for transcriptional cis regulation of Nanog gene expression. Mol Cell Biol 25:2475–2485.

Labosky PA, Barlow DP, Hogan BL. 1994. Embryonic germ cell lines and their derivation from mouse primordial germ cells. Ciba Found Symp 182:157–168, discussion 168–178.

Lavrrar JL, Farnham PJ. 2004. The use of transient chromatin immunoprecipitation assays to test models for E2F1-specific transcriptional activation. J Biol Chem 279:46343–46349.

Lee JH, Hart SR, Skalnik DG. 2004. Histone deacetylase activity is required for embryonic stem cell differentiation. Genesis 38:32–38.

Lim LS, Loh YH, Zhang W, Li Y, Chen X, Wang Y, Bakre M, Ng HH, Stanton LW. 2007. Zic3 is required for maintenance of pluripotency in embryonic stem cells. Mol Biol Cell 18:1348–1358.

Loh YH, Wu Q, Chew JL, Vega VB, Zhang W, Chen X, Bourque G, George J, Leong B, Liu J, Wong KY, Sung KW, Lee CW, Zhao XD, Chiu KP, Lipovich L, Kuznetsov VA, Robson P, Stanton LW, Wei CL, Ruan Y, Lim B, Ng HH. 2006. The Oct4 and Nanog transcription network regulates pluripotency in mouse embryonic stem cells. Nat Genet 38:431–440.

Martin GR. 1981. Isolation of a pluripotent cell line from early mouse embryos cultured in media conditioned by teratocarcinoma stem cells. Proc Natl Acad Sci USA 78:7634–7638.

Meshorer E, Yellajoshula D, George E, Scambler PJ, Brown DT, Misteli T. 2006. Hyperdynamic plasticity of chromatin proteins in pluripotent embryonic stem cells. Dev Cell 10:105–116.

Mitsui K, Tokuzawa Y, Itoh H, Segawa K, Murakami M, Takahashi K, Maruyama M, Maeda M, Yamanaka S. 2003. The homeoprotein Nanog is required for maintenance of pluripotency in mouse epiblast and ES cells. Cell 113:631–642.

Muta M, Kamachi Y, Yoshimoto A, Higashi Y, Kondoh H. 2002. Distinct roles of SOX2, Pax6 and Maf transcription factors in the regulation of lens-specific delta1-crystallin enhancer. Genes Cells 7:791–805.

Nichols J, Zevnik B, Anastassiadis K, Niwa H, Klewe-Nebenius D, Chambers I, Scholer H, Smith A. 1998. Formation of pluripotent stem cells in the mammalian embryo depends on the POU transcription factor Oct4. Cell 95:379–391.

Nishimoto M, Fukushima A, Okuda A, Muramatsu M. 1999. The gene for the embryonic stem cell coactivator UTF1 carries a regulatory element which selectively interacts with a complex composed of Oct-3/4 and Sox-2. Mol Cell Biol 19:5453–5465.

Okita K, Ichisaka T, Yamanaka S. 2007. Generation of germline-competent induced pluripotent stem cells. Nature 448:313–317.

Okumura-Nakanishi S, Saito M, Niwa H, Ishikawa F. 2005. Oct-3/4 and Sox2 regulate Oct-3/4 gene in embryonic stem cells. J Biol Chem 280:5307–5317.

Pesce M, Scholer HR. 2001. Oct-4: Gatekeeper in the beginnings of mammalian development. Stem Cells 19:271–278.

Resnick JL, Bixler LS, Cheng L, Donovan PJ. 1992. Long-term proliferation of mouse primordial germ cells in culture. Nature 359:550–551.

Rodda DJ, Chew JL, Lim LH, Loh YH, Wang B, Ng HH, Robson P. 2005. Transcriptional regulation of nanog by OCT4 and SOX2. J Biol Chem 280: 24731–24737.

Rossant J. 2007. Stem cells and lineage development in the mammalian blastocyst. Reprod Fertil Dev 19:111–118.

Shamblott MJ, Axelman J, Wang S, Bugg EM, Littlefield JW, Donovan PJ, Blumenthal PD, Huggins GR, Gearhart JD. 1998. Derivation of pluripotent stem cells from cultured human primordial germ cells. Proc Natl Acad Sci USA 95:13726–13731.

Spallotta F, Rosati J, Straino S, Nanni S, Grasselli A, Ambrosino V, Rotili D, Valente S, Farsetti A, Mai A, Capogrossi MC, Gaetano C, Illi B. 2010. Nitric oxide determines mesodermic differentiation of mouse embryonic stem cells by activating class IIa histone deacetylases: Potential therapeutic implications in a mouse model of hindlimb ischemia. Stem Cells 28:431–442.

Takahashi K, Yamanaka S. 2006. Induction of pluripotent stem cells from mouse embryonic and adult fibroblast cultures by defined factors. Cell 126:663–676.

Thomson JA, Itskovitz-Eldor J, Shapiro SS, Waknitz MA, Swiergiel JJ, Marshall VS, Jones JM. 1998. Embryonic stem cell lines derived from human blastocysts. Science 282:1145–1147.

Tokuzawa Y, Kaiho E, Maruyama M, Takahashi K, Mitsui K, Maeda M, Niwa H, Yamanaka S. 2003. Fbx15 is a novel target of Oct3/4 but is dispensable for embryonic stem cell self-renewal and mouse development. Mol Cell Biol 23:2699–2708.

Tomioka M, Nishimoto M, Miyagi S, Katayanagi T, Fukui N, Niwa H, Muramatsu M, Okuda A. 2002. Identification of Sox-2 regulatory region which is under the control of Oct-3/4-Sox-2 complex. Nucleic Acids Res 30:3202–3213.

Wang AH, Yang XJ. 2001. Histone deacetylase 4 possesses intrinsic nuclear import and export signals. Mol Cell Biol 21:5992–6005.

Wang AH, Kruhlak MJ, Wu J, Bertos NR, Vezmar M, Posner BI, Bazett-Jones DP, Yang XJ. 2000. Regulation of histone deacetylase 4 by binding of 14-3-3 proteins. Mol Cell Biol 20:6904–6912.

Wang ZX, Teh CH, Kueh JL, Lufkin T, Robson P, Stanton LW. 2007. Oct4 and Sox2 directly regulate expression of another pluripotency transcription factor, Zfp206, in embryonic stem cells. J Biol Chem 282:12822–12830.

Watt TJ, Doyle DF. 2005. ESPSearch: A program for finding exact sequences and patterns in DNA, RNA, or protein. Biotechniques 38:109–115.

Weinmann AS, Yan PS, Oberley MJ, Huang TH, Farnham PJ. 2002. Isolating human transcription factor targets by coupling chromatin immunoprecipitation and CpG island microarray analysis. Genes Dev 16:235–244.

Wells J, Farnham PJ. 2002. Characterizing transcription factor binding sites using formaldehyde crosslinking and immunoprecipitation. Methods 26:48–56.

Yu J, Vodyanik MA, Smuga-Otto K, Antosiewicz-Bourget J, Frane JL, Tian S, Nie J, Jonsdottir GA, Ruotti V, Stewart R, Slukvin II, Thomson JA. 2007. Induced pluripotent stem cell lines derived from human somatic cells. Science 318:1917–1920.

Zappone MV, Galli R, Catena R, Meani N, De Biasi S, Mattei E, Tiveron C, Vescovi AL, Lovell-Badge R, Ottolenghi S, Nicolis SK. 2000. Sox2 regulatory sequences direct expression of a (beta)-geo transgene to telencephalic neural stem cells and precursors of the mouse embryo, revealing regionalization of gene expression in CNS stem cells. Development 127: 2367–2382.